# Floquet non-equilibrium Green's function and Floquet quantum master equation for electronic transport: The role of electron-electron interactions

Vahid Mosallanejad, <sup>1,\*</sup> Yu Wang, <sup>1</sup> and Wenjie Dou<sup>1,†</sup>

<sup>1</sup>Department of Chemistry, Westlake University, Hangzhou,
Zhejiang 310024, China & Institute of Natural Sciences,
Westlake Institute for Advanced Study, Hangzhou, Zhejiang 310024, China
(Dated: October 31, 2023)

Non-equilibrium Green's function (NEGF) and quantum master equation (QME) are two main classes of approaches for electronic transport. We discuss various Floquet variances of these formalisms for transport properties of a quantum dot driven via interaction with an external periodic field. We first derived two versions of the Floquet NEGF. We also explore an ansatz of the Floquet NEGF formalism for the interacting systems. In addition, we derived two versions of Floquet QME in the weak interaction regime. With each method, we elaborate on the evaluation of the expectation values of the number and current operators. We examined these methods for transport through a two-level system that is subject to periodic driving. The results of all four methods show great consistency. We expect these Floquet quantum transport methods to be useful in studying molecular junctions exposed to light.

## I. INTRODUCTION

Light-matter interactions on quantum scales have long been an attractive research topic[1]. In particular, strong electron-photon interaction opens a new avenue toward engineering material properties [2, 3]. In the interpretation of phenomena related to light-matter interaction, the strength of light plays an essential role such that a perturbative treatment of light-matter interaction becomes insufficient [4]. Technological advancements, for example, in time-resolved photo spectroscopy [5], have allowed us to experimentally demonstrate exotic states such as Floquet-Bloch states on topological insulators [6, 7]. Electronic states in such a system can be understood via Floquet theory as if a classical monochromatic light is coupled to a closed fermionic system [8, 9]. Floquet theory is a non-perturbative mathematical technique that essentially turns the time-dependent schrödinger equation with a time-periodic Hamiltonian to a time-independent equation in the price of increasing the dimensionality of the basis set [10, 11]. Floquet theory has been used in the interpretation of Kondo effects, and noise effects [12, 13], spin currents in DNA [14], electron transfer in donor-bridge-acceptor systems [15], driven quantum dots [16, 17], laser absorption properties[18], nonadiabatic dynamics [19] and many other applications.

To further enhance our understanding of light-matter interactions, it seems essential to develop approaches that describe how light interacts with open quantum systems. This requirement can be met by properly combining the Floquet theory with quantum transport theories. In other words, two classes of quantum transport approaches, namely the non-equilibrium Green's function (NEGF) and the quantum master equation (QME),

can be complemented with the Floquet theory. There have been several works on extending the Floquet theory to open quantum systems. Floquet Green's function is defined in a number of different ways [20–23]. While the Floquet QME was less well-established in the past [13, 24], recent demands for dynamically controlling the material properties by the Floquet engineering stimulated the development of new methods [25–31].

NEGF approaches are often employed when a onebody Hamiltonian (e.g., the tight-binding Hamiltonian) can sufficiently describe a system of interest (the dot) whereas QME is suitable when many-body interactions (such as electron-electron Coulomb repulsion) are important [32]. In addition, QME is known to work well when the coupling between the System and environment is weak (weak-coupling limit) whereas NEGF is insensitive to the System-environment coupling strength. Historically, two main flavors for Floquet theory exist in the context of quantum mechanics/solid state physics. The first one that focused on the evolution operator was developed by Shirley in the mid-sixties [33] while the second one that focused on the discreet expansion of wavefunction was developed by Sambe [10]. In this work, we intend to discuss that there are multiple ways in which both quantum transport approaches can benefit from the Floquet theory.

We will offer compact derivations for Floquet non-equilibrium Green's functions (which rely on the expansion of Green's function pioneered by Sambe) and we will also microscopically derive two versions of Floquet quantum master equations (one based on the Floquet-based evolution operator pioneered by Shirley and the other relies on the concept of Floquet density matrix). We will also examine presented methods for a model system. To the best of our knowledge, there is no work dedicated to the consistency check between different Floquet quantum transport theories. Here, we sketch general Floquet theories which are neither based on an average Hamiltonian approach (Floquet-Magnus) nor based on stroboscopic

<sup>\*</sup> vahid@westlake.edu.cn

<sup>†</sup> douwenjie@westlake.edu.cn

and micromotion evolution (Van Vleck approximation) [34]. Hence, the approaches presented here are not sensitive to the value of driving frequency, in principle.

#### II. THEORY

#### A. Model Hamiltonian

With this work, we are concerned with the electronic transport through a quantum dot (the System) that is weakly connected to the thermal fermionic bath (lead) while it strongly interacts with an external monochromatic light with the frequency  $\omega$ . In such scenarios, often a time-periodic off-diagonal term (that represents the dipole approximation) should be added to the unperturbed System Hamiltonian ( $\hat{H}_S$ ) such that the total System Hamiltonian will become time-periodic  $\hat{H}_S(t) = \hat{H}_S(t+T)$  [ $T=2\pi/\omega$ ]. The bath Hamiltonian,  $\hat{H}_B$ , and the system-bath interaction,  $\hat{H}_{SB}$ , will be remained time-independent. The spinless model Hamiltonian can be given by

$$\hat{H}_{tot}(t) = \hat{H}_S(t) + \hat{H}_B + \hat{H}_{SB}$$
 (1)

$$\hat{H}_S(t) = \sum_{i,j} h_{ij}(t) \hat{d}_i^{\dagger} \hat{d}_j \tag{2}$$

$$\hat{H}_B = \sum_{lk} \epsilon_{lk} \hat{c}_{lk}^{\dagger} \hat{c}_{lk} \tag{3}$$

$$\hat{H}_{SB} = \sum_{ll,i} V_{lk,i} \hat{c}_{lk}^{\dagger} \hat{d}_i + \text{H.c.}$$
 (4)

Here,  $\hat{d}_i$  ( $\hat{d}_i^{\dagger}$ ) is the System's electronic annihilation (creation) operator in the many-body space and  $h_{ij}(t) = h_{ij}(t+T)$  represents a periodic one-body Hamiltonian. Likewise,  $\hat{c}_{lk}$  ( $\hat{c}_{lk}^{\dagger}$ ) is the annihilation (creation) operator for the kth electronic orbital in the bath l. The quantity  $V_{lk,i}$  is the coupling strength between the kth orbital of the bath (lead) l, and the System's orbital  $\hat{d}_i$ . In addition the number operator is  $\hat{n} = \sum_i \hat{d}_i^{\dagger} \hat{d}_i$ . We can further simplify the notation of system-bath interaction Hamiltonian as  $\hat{H}_{SB} = \sum_i \hat{C}_i^{\dagger} \hat{d}_i + \text{H.c.}$  We shall also associate the bath l with the electrochemical potential  $\mu_l$ . Note that the System Hamiltonian is quadratic whereas the bath Hamiltonian is non-interacting.

# B. Floquet Green's function

In the following we explore two types of Floquet Green's function whereby we named 1) Vector-like NEGF, and 2) Matrix-like NEGF. Our starting point for deriving these two flavors of Floquet Green's function is the two-time Kadanoff-Baym (KB) equation [35, 36] for

the retarded Green's function,  $G^r(t, t')$ , as

$$\left(i\frac{d}{dt} - h(t)\right)G^r(t, t') - \int_{-\infty}^{+\infty} dt_1 \Sigma^r(t, t_1) \times G^r(t_1, t') = I\delta(t - t').$$
(5)

Hereafter, we will set  $\hbar = 1$ .  $\Sigma^r = \sum_l \Sigma_l^r$  refers to the total retarded self-energy.  $\Sigma_l^r$  refers to the retarded self-energy of the non-interacting bath l, which only depends on the time difference, such that  $\Sigma^r(t,t') = \Sigma^r(t-t')$ .

# 1. Vector-like (V-like) Floquet NEGF

One way to derive the EOM within the V-like Floquet NEGF is to split the derivation into two parts. In the first part, we define following time-energy retarded and advanced Green's functions

$$\int_{-\infty}^{\infty} dt' G^{r/a}(t, t') e^{i\mathcal{E}(t-t')} = G^{r/a}(t, \mathcal{E}), \tag{6}$$

where  $\mathcal{E}$  is the quasi-energy variable. Then, after performing the continuous Fourier transformation, the KB equation for retarded Green's function simplifies as

$$\left(\mathcal{E}I + i\frac{d}{dt} - h(t)\right)G^{r}(t,\mathcal{E}) - \int_{0}^{+\infty} d\tau \Sigma^{r}(\tau) \times e^{\frac{i\mathcal{E}}{\hbar}\tau}G^{r}(t-\tau,\mathcal{E}) = I$$
(7)

Note that  $\tau = t - t_1$ , and we have employed *convolution* identity in the self-energy term. In the second part, we expand the  $G^r(t,\mathcal{E})$  with the following complex Fourier series

$$G^{r}(t,\mathcal{E}) = \sum_{n=-N}^{N} e^{-in\omega t} g_n^{r}(\mathcal{E}).$$
 (8)

N is an integer that determines the truncation of the Fourier space basis set. After substitution Eq. (8) into Eq. (7), we arrive at

$$\sum_{n} \left( e^{-in\omega t} \mathcal{E} I + e^{-in\omega t} n\omega I - h(t) e^{-in\omega t} \right) g_n^r(\mathcal{E}) -$$

$$\sum_{n} e^{-in\omega(t)} \int_0^{+\infty} d\tau \Sigma^r(\tau) e^{i(\mathcal{E} + n\omega)\tau} g_n^r(\mathcal{E}) = I.$$
(9)

We then desire to find an EOM for  $g_n^r(\mathcal{E})$  which requires multiplying both sides to  $e^{im\omega t}$  and taking the time average over one period. EOM for  $g_n^r(\mathcal{E})$  reads as

$$\left( \left( (\mathcal{E} + m\omega)I - \bar{\Sigma}^r (\mathcal{E} + m\omega) \right) \delta_{mn} - \sum_n h_{mn} \right) \times 
g_n^r(\mathcal{E}) = \delta_{m0}I,$$
(10)

where  $\bar{\Sigma}^r$  and  $[h]_{mn}$  are given by

$$\bar{\Sigma}^r(\mathcal{E} + m\hbar\omega) = \int_0^{+\infty} d\tau \Sigma^r(\tau) e^{i(\mathcal{E} + m\omega)\tau}, \quad (11)$$

$$h_{mn} = \frac{1}{T} \int_0^T dt e^{im\omega t} h(t) e^{-in\omega t}. \quad (12)$$

By running Eq. (10) over indices n and m, the compact form of V-like Floquet NEGF appears as

$$\left(\mathcal{E}[I^F] - [h^F] - [\bar{\Sigma}^{rF}]\right) \mathbf{g}^{rF}(\mathcal{E}) = \mathbf{I}_o^F, \tag{13}$$

where the  $[h^F] = \sum_{n,m} h_{mn} - I(m\omega)\delta_{mn}$  is a standard definition for the Floquet Hamiltonian.  $[I^F]$  and  $[\bar{\Sigma}^{r/a}^F]$  are block diagonal matrices made of I and  $\bar{\Sigma}^{r/a}$ . In the above block matrix EOM, the  $\mathbf{g}^{rF}$  refers to a stack of  $g_n^r$  placed over each other (V-like), and  $\mathbf{I}_o^F$  refers to a stacking zero matrices symmetrically placed around a central identity matrix. Note that with the energy-independent wide-band approximation,  $\bar{\Sigma}^r(\mathcal{E}+m\omega)=\bar{\Sigma}^r$ , there would be no implementation complexity on the Floquet self-energy term. In addition,  $\mathcal{E}$  is unbounded. The most important point about Eq. (13) is that it is a time-independent EOM. Such a two step procedure was first employed by Sambe to directly solve Schrödinger equation with the time-periodic Hamiltonian. Also, one can combine the inverse of Eq. (6) with Eq. (8) to expand the two-time quantity Q(t,t') in the V-like form as

$$Q(t,t') = \sum_{n} \int_{-\infty}^{\infty} \frac{d\mathcal{E}}{2\pi} e^{-i(\mathcal{E} + n\omega)t} e^{i\mathcal{E}t'} q_n(\mathcal{E}).$$
 (14)

From the definition given in Eq. (14), the requirement  $G^a(t',t) = G^r(t,t')^{\dagger}$  indicates  $g_n^a(\mathcal{E}) = g_{-n}^r(\mathcal{E} + n\omega)^{\dagger}$ .

## 2. Matrix-like (M-like) Floquet NEGF

We first define the following one-step transformation for a two-time function

$$Q(t,t') = \sum_{n,m} \int_0^\omega \frac{d\mathcal{E}}{2\pi} e^{-i(\mathcal{E}+n\omega)t} e^{i(\mathcal{E}+m\omega)t'} q_{nm}(\mathcal{E}).$$
 (15)

The inverse transformation, for the matrix coefficients  $q_{nm}(\mathcal{E})$ , is given by

$$q_{nm}(\mathcal{E}) = \int_{-\infty}^{\infty} \frac{dt'}{T} \int_{0}^{T} dt e^{i(\mathcal{E} + n\omega)t} e^{-i(\mathcal{E} + m\omega)t'} Q(t, t'). \quad (16)$$

Contrary to V-like Floquet NEGF,  $\mathcal{E}$  is a bounded (independent) variable on the range  $[0\ \omega]$ . We proceed by expanding  $G^r$  using Eq. (15) and substituting the result into the KB equation, and solving for the matrix coefficient  $g_{nm}^r$ . In this process, one can first notice that RHS can be reduced to  $I\delta_{nm}$ . After some lengthy algebra, we arrive at the following EOM for the retarded Green's

$$\left( (\mathcal{E} + n\omega) - \bar{\Sigma}^r (\mathcal{E} + n\omega) \right) g_{nm}^r (\mathcal{E}) - 
\sum_k h_{nk} g_{km}^r (\mathcal{E}) = I \delta_{nm}.$$
(17)

The definition of  $\bar{\Sigma}^r$  and  $h_{nk}$  is identical to what is given in Eqs. (11) and (12). Comparing Eq. (10) with Eq.

(17), it is evident why this form of EOM can be referred to as the Matrix-like Floquet NEGF. The compact form of M-like Floquet Green's function reads as

$$\left(\mathcal{E}[I^F] - [h^F] - [\bar{\Sigma}^{rF}]\right)[G^{rF}](\mathcal{E}) = [I^F]. \tag{18}$$

In the M-like framework, the condition  $G^a(t',t)=G^r(t,t')^\dagger$  imposes  $g^a_{nm}=(g^r_{mn})^\dagger$  which in turn confirms that  $[G^{a\,F}]=[G^{r\,F}]^\dagger$ . This property makes the M-like framework more convenient compared to the V-like.

# C. Observable in Floquet NEGF

To explore the transport properties, the expectation values of two (operators) observable are essential. 1) the number operator  $\langle \hat{n} \rangle (t)$ , and 2) the terminal current  $\langle \hat{J} \rangle = J$ . For  $\langle \hat{n} \rangle (t)$ , we shall trace the two-time lesser Green's function as  $\langle \hat{n} \rangle (t) = -i \operatorname{Tr}(G^{<}(t,t))$  [36]. The  $G^{<}(t,t')$  given by

$$G^{<}(t,t') = \int_{-\infty}^{+\infty} dt_1 \int_{-\infty}^{+\infty} dt_2 G^r(t,t_1) \times \sum_{=\infty}^{\infty} (t_1 - t_2) G^a(t_2,t').$$
(19)

The total lesser self-energy is denoted by:  $\Sigma^{<} = \sum_{l} \Sigma_{l}^{<}$ . The two-time particle current per spin passing through the contact l is given by

$$J_{l}(t,t') = \int_{-\infty}^{+\infty} dt_{1} \Big( G^{r}(t,t_{1}) \Sigma_{l}^{<}(t_{1},t') + G^{<}(t,t_{1}) \Sigma_{l}^{a}(t_{1},t') \Big).$$
(20)

In the following (without details of derivation), we summarize general expressions for Floquet components of these two observable within the V-like and M-like Floquet NEGF frameworks.

Observable in the V-like Floquet NEGF.— The expansion given in Eq. (14) will be used to expand  $G^{</r/a}$  (in terms of  $g_n^{</r/a}$ ) and resulting expressions will be substituted in Eq. (19). Then, we proceed to derive the matrix coefficients  $g_n^{<}(\mathcal{E})$ . After doing some algebra, it reads as

$$g_n^{<}(\mathcal{E}) = \sum_{m} g_{n-m}^r(\mathcal{E} + m\omega) \Sigma^{<}(\mathcal{E} + m\omega) g_m^a(\mathcal{E}) = \sum_{m} g_{n-m}^r(\mathcal{E} + m\omega) \Sigma^{<}(\mathcal{E} + m\omega) g_{-m}^r(\mathcal{E} + m\omega)^{\dagger}.$$
(21)

In the energy domain, the lesser self-energy is:  $\bar{\Sigma}_l^{<}(\mathcal{E}) = i\Gamma_l^r(\mathcal{E})f_l(\mathcal{E}), \ \Gamma_l^r = 2\operatorname{Im}(\bar{\Sigma}_l^r).$  Here,  $f_l(\mathcal{E}) \equiv f(\mathcal{E}, \mu_l)$  and  $\mu_l$  are the Fermi function and the electrochemical potential associated with the terminal l.

For the *current*, we will follow the same procedure with expanding the  $J_l(t,t')$  in terms of the matrix coefficient  $J_{l,n}(\mathcal{E})$ . Solving for  $J_{l,n}(\mathcal{E})$ , we arrive at

$$J_{l,n}(\mathcal{E}) = \left(g_n^r(\mathcal{E})\bar{\Sigma}_l^{<}(\mathcal{E}) + g_n^{<}(\mathcal{E})\bar{\Sigma}_l^a(\mathcal{E})\right). \tag{22}$$

Observable in the M-like Floquet NEGF.– Similar to above, one can employ Eq. (15) to expand  $G^{</a/r}$  and substitute the resulting expressions in Eq. (19). After doing some algebra, we arrive at the following relation for  $g_{nm}^{<}(\mathcal{E})$ 

$$g_{nm}^{<}(\mathcal{E}) = \sum_{k} g_{nk}^{r}(\mathcal{E}) \bar{\Sigma}^{<}(\mathcal{E} + m\omega) g_{km}^{a}(\mathcal{E}). \tag{23}$$

For the *current*,  $J_l(t, t')$  has to be expanded in terms of the coefficient matrix  $J_{l,nm}(\mathcal{E})$  using Eq. (15). Substituting expanded forms of all components into Eq. (19) and solving for  $J_{l,nm}(\mathcal{E})$  results in

$$J_{l,nm}(\mathcal{E}) = \left(g_{nm}^r(\mathcal{E})\bar{\Sigma}_l^{<}(\mathcal{E} + m\omega) + g_{nm}^{<}(\mathcal{E})\bar{\Sigma}_l^a(\mathcal{E} + m\omega)\right).$$
(24)

Eqs. (21-24) may look complex at first glance, however, these equations can be further simplified when we evaluate the time-averaged of an observable.

### D. Time-average of an observable

Within the V-like Floquet NEGF framework, the time average of an observable over one period can be obtained by changing the t' to t in Eq. (14) and performing the time average over one period. Using Eq. (21), the time average of the number operator over one period,  $\overline{n}$ , in the V-like framework read as

$$\overline{n} = \frac{-i}{T} \int_0^T dt \operatorname{Tr}(G^{<}(t,t)) = -i \int_{-\infty}^{\infty} \frac{d\mathcal{E}}{2\pi} \operatorname{Tr}(g_0^{<}(\mathcal{E}))$$

$$= -i \int_{-\infty}^{\infty} \frac{d\mathcal{E}}{2\pi} \sum_m \operatorname{Tr}\left(g_m^r(\mathcal{E})\bar{\Sigma}^{<}(\mathcal{E} + m\omega)g_m^r(\mathcal{E})^{\dagger}\right). \tag{25}$$

In the above expression, we have used the property  $g^r_{-m}(\mathcal{E}+m\omega)=g^r_{m}(\mathcal{E})$ , and we have also employed the wide-band approximation as well. We stress that only the central component (n=0) of  $\mathbf{g}^<$  is required to evaluate the time average of  $\langle \hat{n} \rangle (t)$  over one period.

Within the M-like Floquet NEGF framework, the time average of the number operator over one period reads as

$$\overline{n} = -i \sum_{n} \int_{0}^{\omega} \frac{d\mathcal{E}}{2\pi} \operatorname{Tr}(g_{nn}^{<}(\mathcal{E}))$$

$$= -i \int_{0}^{\omega} \frac{d\mathcal{E}}{2\pi} \operatorname{Tr}\left([G^{rF}](\mathcal{E})[\bar{\Sigma}^{
(26)$$

Here,  $[\bar{\Sigma}^{< F}](\mathcal{E})$  denotes a block diagonal matrix made of  $\bar{\Sigma}^{<}(\mathcal{E} + m\omega)$ .

Next, we simplify current expressions. In the V-like framework, the time average of the current over a period,  $\overline{J}$ , simplifies as

$$\overline{J}_{l} = -i \int_{-\infty}^{\infty} \frac{d\mathcal{E}}{2\pi} \Big( g_{0}^{r}(\mathcal{E}) \Sigma_{l}^{<}(\mathcal{E}) + g_{0}^{<}(\mathcal{E}) \Sigma_{l}^{a}(\mathcal{E}) \Big). \quad (27)$$

In the M-like framework, based on Eqs. (15) and (24), the time average of the current over one period read as

$$\overline{J}_{l} = -i \sum_{n} \int_{0}^{\omega} \frac{d\mathcal{E}}{2\pi} \operatorname{Tr}(J_{l,nn}(\mathcal{E}))$$

$$= -i \int_{0}^{\omega} \frac{d\mathcal{E}}{2\pi} \operatorname{Tr}\left( [G^{rF}](\mathcal{E})[\bar{\Sigma}_{l}^{
(28)$$

In the absence of electron-electron interaction, same as in none-Floquet scenarios, the above relation can be further simplified to a Landauer-like expression for a twoterminal device as

$$\overline{J}_{l} = \int_{0}^{\omega} \frac{d\mathcal{E}}{2\pi} T_{ll'}(\mathcal{E}) (f_{l} - f_{l'}), 
T_{ll'}(\mathcal{E}) = \text{Tr} \left( [\overline{\Gamma}_{l}^{rF}] [G^{rF}] (\mathcal{E}) [\overline{\Gamma}_{l'}^{rF}] [G^{rF}]^{\dagger} (\mathcal{E}) \right),$$
(29)

where  $T_{ll'}(\mathcal{E})$  is the two terminal transmission function. Here,  $[\bar{\Gamma}_{l/l'}^{rF}]$  is the block diagonal matrix made of  $\bar{\Gamma}_{l/l'}^{r}$ .

#### E. Floquet Green's function for interacting systems

For interaction systems, we introduce an ansatz for the M-like Floquet Green's function related to the equation-of-motion method [37]. We should consider the spin degree of freedom in the total Hamiltonian, Eqs. (1)-(4), by modifying annihilation (creation) operators  $\hat{d}_i^{(\dagger)}/\hat{c}_{i,\sigma}^{(\dagger)} \to \hat{d}_{i,\sigma}^{(\dagger)}/\hat{c}_{i,\sigma}^{(\dagger)}$  in which  $\sigma=\uparrow,\downarrow$ . The (time-independent) electron-electron interaction,  $\hat{H}_{ee}$ , is given by a Hubbard-like two-body interaction as

$$\hat{H}_{ee} = \sum_{i} u_i \, \hat{d}_{i,\sigma}^{\dagger} \hat{d}_{i,\sigma} \hat{d}_{i,\tilde{\sigma}}^{\dagger} \hat{d}_{i,\tilde{\sigma}}. \tag{30}$$

Here,  $\tilde{\sigma}$  refers to opposite spin of  $\sigma$ . In case of time-independent  $h_{ij}$  (None-Floquet case) and with truncating to double-particle Green's function,  $G^{(2)r}(\mathcal{E})$ , one can obtain a close form for the retarded Green's function as

$$\left(\mathcal{E}[I] - [h] - [\bar{\Sigma}_{\sigma}^r]\right) [G_{\sigma}^r](\mathcal{E}) = [I] + [U][G_{\sigma}^{(2)r}](\mathcal{E}), (31)$$

$$\left(\mathcal{E}[I] - [h] - [U] - [\bar{\Sigma}_{\sigma}^r]\right) [G_{\sigma}^{(2)r}](\mathcal{E}) = [\langle n_{\tilde{\sigma}} \rangle], \qquad (32)$$

where, [U] refers to a diagonal matrix consist of the elements  $\{u_i\}$ . The matrix  $[\langle n_{\tilde{\sigma}} \rangle]$  is a diagonal matrix consist of occupation numbers  $\langle n_{i\tilde{\sigma}} \rangle$ . Although, Eqs. (31) and (32) suggest a self-consistent procedure but  $\langle n_{i\tilde{\sigma}} \rangle = 1/2$  gives a good quantitative prediction on the onsets of current plateaus (charging effects) related to the coulomb blockade phenomenon. In previous sections where we discussed the Floquet transformation, we saw that the none time-dependent components of Green's function equation turn into fixed diagonal blocks. Here, we extend this observation to the interacting case, and hence, we expect the following M-like Floquet version for

the Eqs. (31)-(32) as

$$\begin{split} & \left( \mathcal{E}[I^F] - [h^F] - [\bar{\Sigma}_{\sigma}^{rF}] \right) [G_{\sigma}^{rF}] = [I^F] + [U^F] [G_{\sigma}^{(2)rF}], \\ & \left( \mathcal{E}[I^F] - [h^F] - [U^F] - [\bar{\Sigma}_{\sigma}^{rF}] \right) [G_{\sigma}^{(2)rF}] = [\langle n_{\tilde{\sigma}} \rangle^F]. \end{split}$$

In addition, based on the EOM technique and the above argument, we would have also the following expressions for the M-like Floquet lesser Green's functions

$$\left(\mathcal{E}[I^F] - [h^F] - [\bar{\Sigma}_{\sigma}^{

$$\left[U^F\right][G_{\sigma}^{(2)

$$\left(\mathcal{E}[F] - [h^F] - [\bar{\Sigma}_{\sigma}^{
(35)$$$$$$

$$\left(\mathcal{E}[I^F] - [h^F] - [U^F] - [\bar{\Sigma}_{\sigma}^{rF}]\right) [G_{\sigma}^{(2) < F}] = 
[\Gamma_{\sigma}^{
(36)$$

Note that, the lesser Green's function for the interacting case is different than the none-interacting one. Consequently, the expectation value of the number operator and the average of the number operator over one period should follow Eq. (35). However, the expression for the average current per cycle is identical to the non-interacting case. It is worth mentioning that the Landauer formula is not correct in the case of interacting systems and hence there would be no Landauer-like expression for the average current per cycle.

#### F. Floquet Quantum Master Equation

In the following we explore two types of Floquet Quantum Master Equation (FQME) whereby we named 1) Hilbert-Space FQME (HS-FQME), and 2) Floquet-Space FQME (FS-FQME). Our starting point for deriving HS-FQME is the well-known Redfield QME in the Schrödinger picture whereas we will start from the Floquet Liouville von-Neumann (FLvN) equation for deriving HS-FQME.

## 1. Hilbert-Space FQME

When the Hamiltonian of the System is time-dependent (not restricted to the time-periodic), the dynamics of the System's density operator can be notified by the following Redfield equation

$$\frac{\partial \hat{\rho}_{S}(t)}{\partial t} = -i \left[ \hat{H}_{S}(t), \hat{\rho}_{S}(t) \right] - 
\int_{0}^{\infty} \operatorname{Tr}_{B} \left[ \hat{H}_{SB}, \left[ \tilde{\tilde{H}}_{SB}(t, \tau), \hat{\rho}_{S}(t) \otimes \hat{\rho}_{B} \right] \right] d\tau,$$

$$\tilde{\tilde{H}}_{SB}(t, \tau) = \sum_{i} \tilde{\tilde{C}}_{i}^{\dagger}(\tau) \tilde{\tilde{d}}_{i}(t, \tau) + \tilde{\tilde{d}}_{i}^{\dagger}(t, \tau) \tilde{\tilde{C}}_{i}(\tau)$$
(38)

where  $\hat{\rho}_S(t)$  and  $\hat{\rho}_B$  are the System and bath manybody density operators.  $\text{Tr}_B$  indicates tracing over the bath degrees of freedom. In the, Eq. (38),  $\tilde{\tilde{C}}_i(\tau) =$   $\sum_{lk} V_{lk,i}^* \hat{c}_{lk} e^{i\,\epsilon_{lk}\tau}$  and it determines how the bath part of the  $\hat{H}_{SB}$  evolve in the bath's time scale,  $\tau$ . On the other hand,  $\tilde{d}_i(t,\tau) = \hat{U}_S(t,t-\tau)\hat{d}_i\hat{U}_S^{\dagger}(t,t-\tau)$  describes the evolution of the System part of the  $\hat{H}_{SB}$  in which the time evolution operator is  $\hat{U}_S(t,t-\tau) = \mathcal{T}exp\left(-i\int_{t-\tau}^t \hat{H}_S(s)ds\right)$  ( $\mathcal{T}$  refers to the time-ordering operator). Same definition holds for  $\tilde{d}_i^{\dagger}(t,\tau)$ . It was Shirley who first formalized the time evolution operator for the time-periodic Hamiltonian. The time evolution operator can be expressed as

$$\hat{U}_S(t, t_0) = \sum_{n} \langle n | e^{-i\hat{H}_S^F(t - t_0)} | 0 \rangle e^{in\omega t}, \tag{39}$$

where  $|n\rangle$  ( $|0\rangle$ ) refers to the *n*th (0th) state in the Fourier basis set. Here, the Floquet many-body Hamiltonian defines identical to the one-body counterpart as  $\hat{H}_S^F = \sum_{n,m} \hat{H}_{S\,mn} - \hat{I}(m\omega)\delta_{mn}$  in which  $\hat{H}_{S\,mn}$  defines similar to Eq. (12). In general, disassembling the double commutator in Eq. (37) results in eight major integrands. In addition, having two parts in Eq. (38) results in a total of sixteen integrands. From these, only eight integrands should be considered (terms in which one of the operators multiples to the conjugate transpose of the other). For example, the first and second non-vanishing terms (*Dissipators*) can be given as

$$\sum_{i,j} \int_{0}^{\infty} \operatorname{Tr}_{B} \left( \left( \hat{C}_{i}^{\dagger} \hat{d}_{i} + \hat{d}_{i}^{\dagger} \hat{C}_{i} \right) \left( \tilde{\tilde{C}}_{j}^{\dagger}(\tau) \tilde{\tilde{d}}_{j}(t,\tau) + \tilde{\tilde{d}}_{j}^{\dagger}(t,\tau) \right) \right.$$

$$\left. \tilde{\tilde{C}}_{j}(\tau) \right) \hat{\rho}_{S}(t) \otimes \hat{\rho}_{B} d\tau = \sum_{i,j} \int_{0}^{\infty} \operatorname{Tr}_{B} \left( \hat{C}_{i}^{\dagger} \hat{d}_{i} \tilde{\tilde{d}}_{j}^{\dagger}(t,\tau) \right) \right.$$

$$\tilde{\tilde{C}}_{j}(\tau)\hat{\rho}_{S}(t)\otimes\hat{\rho}_{B}+\hat{d}_{i}^{\dagger}\hat{C}_{i}\tilde{\tilde{C}}_{j}^{\dagger}(\tau)\tilde{\tilde{d}}_{j}(t,\tau)\hat{\rho}_{S}(t)\otimes\hat{\rho}_{B}\Big)d\tau.$$

For the sake of brevity, we only focus on the first Dissipator which can be further simplified to

$$\sum_{i,j} \int_{0}^{\infty} \operatorname{Tr}_{B} \left( \hat{C}_{i}^{\dagger} \tilde{\tilde{C}}_{j}(\tau) \hat{\rho}_{B} \otimes \hat{d}_{i} \tilde{\tilde{d}}_{j}^{\dagger}(t,\tau) \hat{\rho}_{S}(t) \right) d\tau =$$

$$\sum_{i,j,kl} \int_{0}^{\infty} \left( V_{lk,i} V_{lk,j}^{*} e^{i \epsilon_{lk} \tau} f(\epsilon_{lk}, \mu_{l}) \hat{d}_{i} \tilde{\tilde{d}}_{j}^{\dagger}(t,\tau) \hat{\rho}_{S}(t) \right) d\tau.$$

$$(41)$$

Note that  $\operatorname{Tr}_B\left(\hat{c}_{lk}^{\dagger}\hat{c}_{l'k'}\hat{\rho}_B(\mu)\right) = f(\epsilon_{lk},\mu_l)\delta_{k,k'}\delta_{l,l'}$ . Until now, the derivation procedure is not far from the non-Floquet QME. However, complexity in the time dependency of the  $\tilde{d}_j^{\dagger}(t,\tau)$  requires Shirley's Floquet Formalism, Eq. (39), as

$$\tilde{\tilde{d}}_{j}^{\dagger}(t,\tau) = \sum_{n,m} \langle n|e^{-i\hat{H}_{S}^{F}\tau}|0\rangle \hat{d}_{j}^{\dagger}\langle 0|e^{i\hat{H}_{S}^{F}\tau}|m\rangle e^{i(n-m)\omega t}. \quad (42)$$

To proceed, we shall use the eigenbasis of the Floquet System Hamiltonian  $\hat{Y}^{\dagger}\hat{H}_{S}^{F}\hat{Y}=\hat{\Lambda}^{F}$  in which  $\hat{Y}$  is the rotating operator. Then, the above relation can be simplified to

$$\tilde{\tilde{d}}_{j}^{\dagger}(t,\tau) = \sum_{n,m} \langle n | \hat{Y} e^{-i\hat{\Lambda}^{F}\tau} \hat{\mathcal{D}}_{j}^{o\dagger} e^{i\hat{\Lambda}^{F}\tau} \hat{Y}^{\dagger} | m \rangle e^{i(n-m)\omega t}, \quad (43)$$

where  $\hat{\mathcal{D}}_{j}^{o\,\dagger}=\hat{Y}^{\dagger}\big(|0\rangle\hat{d}_{j}^{\dagger}\langle0|\big)\hat{Y}$  and we used the property  $\hat{Y}^{\dagger}\hat{Y}=\hat{I}$  multiple times. Next, we should consider a basis set  $\{|a\rangle\}$  for the Hilbert space which allows us to present elements of density operator as  $\rho_{ab}(t)=\langle a|\hat{\rho}(t)|b\rangle$  and turn operators in Eq. (43) to matrices. In particular, it allows us to work with the (hybrid) Floquet basis,  $\{|\gamma\rangle\}$  such that we can simplify the  $e^{-i\hat{\Lambda}^F\tau}\hat{\mathcal{D}}_{j}^{o\,\dagger}e^{i\hat{\Lambda}^F\tau}$ . A matrix element of this term is given by

$$\left(e^{-i\hat{\Lambda}^F\tau}\hat{\mathcal{D}}_j^{o\dagger}e^{i\hat{\Lambda}^F\tau}\right)_{\gamma,\nu} = e^{-i\Omega_{\gamma\nu}\tau}\left(\hat{\mathcal{D}}_j^{o\dagger}\right)_{\gamma,\nu},\tag{44}$$

where  $\Omega_{\gamma\nu} = (\mathcal{E}_{\gamma} - \mathcal{E}_{\nu})$ . Clear separation of the two time scales (t and  $\tau$ ) allows us to perform the time integration over  $\tau$  as

$$\int_0^\infty e^{i(\epsilon_{lk} - \Omega_{\gamma\nu})\tau} d\tau = \pi \delta(\epsilon_{lk} + \Omega_{\gamma\nu}) - iP(\frac{1}{\epsilon_{lk} + \Omega_{\gamma\nu}}). \quad (4)$$

Neglecting the Cauchy's principle, P, and employing the energy-independent wide-band approximation,  $\Gamma^l_{ij} = 2\pi \sum_k V_{lk,i} V^*_{lk,j}$  results in the following matrix expression for the first Dissipators

$$\sum_{i,j,l} \frac{\Gamma_{ij}^l}{2} d_i \sum_{n,m} \langle n|Y f_l(-\Omega) \circ \mathcal{D}_j^{o\dagger} Y^{\dagger} | m \rangle e^{i(n-m)\omega t} \rho_S(t). \tag{46}$$

where  $\circ$  refers to the Hadamard product. We should repeat this procedure for the other seven non-vanishing Dissipators. A more compact matrix form of the Floquet QME in the Hilbert space can then be given as

$$\frac{\partial \rho_S(t)}{\partial t} = -i \left[ H_S(t), \rho_S(t) \right] - \sum_{i,j,l} \frac{\Gamma_{ij}^l}{2} \left( d_i \widetilde{d}_{jl}^{\dagger}(t) \rho_S(t) + d_i \overline{d}_{jl}(t) \rho_S(t) - d_i \rho_S(t) \widetilde{d}_{il}^{\dagger}(t) - d_i^{\dagger} \rho_S(t) \overline{d}_{jl}(t) \right) + \text{ h.c. },$$
(47)

where  $\widetilde{d}_{il}(t)$  and  $\overline{d}_{il}(t)$  defined as

$$\widetilde{d}_{jl}^{\dagger}(t) = \sum_{n,m} \langle n|Y f_l(-\Omega) \circ \mathcal{D}_j^{o\dagger} Y^{\dagger}|m\rangle e^{i(n-m)\omega t}, \quad (48)$$

$$\overline{d}_{jl}(t) = \sum_{n,m} \langle n|Y f_l(\Omega) \circ \mathcal{D}_j^o Y^{\dagger}|m\rangle e^{i(n-m)\omega t}.$$
 (49)

We stress that within the Hilbert-Space FQME,  $\widetilde{d}_{jl}(t)$  and  $\overline{d}_{jl}(t)$  (and their hermitian conjugates) are time-dependent matrices. Finally, we can simplify the notation of Eq. (47) as  $\partial \rho_S(t)/\partial t = -i \left[H_S(t), \rho_S(t)\right] + \sum_l \mathcal{L}_l^{HS}(t) \rho_S(t)$ .

# 2. Floquet-Space FQME

LvN equation is the starting point for varieties of QMEs (e.g. the Redfield QME). For a periodic Hamiltonian, the LvN equation can be transformed into the Floquet LvN equation which is very general and has a long

history in the analysis of nuclear magnetic resonance signals (closed systems) [11]. The Floquet LvN equation is given by

$$\frac{\partial \hat{\rho}^F(t)}{\partial t} = -i \left[ \hat{H}^F, \hat{\rho}^F(t) \right]$$
 (50)

$$\hat{H}^F = \sum_{n} \hat{L}_n \otimes \hat{H}^{(n)} + \hat{N} \otimes \hat{\mathbf{1}}, \tag{51}$$

$$\hat{H}^{(n)} = \frac{1}{T} \int_0^T dt \, e^{in\omega t} \hat{H}(t) \tag{52}$$

$$\hat{\rho}^F(t) = \sum_n \hat{L}_n \otimes \hat{\rho}^{(n)}(t). \tag{53}$$

Here, n is an integer in the space [-N, N],  $\widehat{L}_n$  is the Ladder operator of the order n,  $\widehat{N}$  is the Number operator in the Fourier space, and  $\widehat{\mathbf{1}}$  is the identity operator in the Hilbert space. In the matrix form,  $\widehat{L}_n$  represents a  $N \times N$  off-diagonal matrix with ones in its off-diagonal and  $\widehat{N}$  represents a diagonal matrix with the integer vector  $\{-N,...,N\}$  placed on it's diagonal. The major benefit of the Floquet LvN equation is that  $\widehat{H}(t)$  turns into a time-independent Hamiltonian  $\widehat{H}^F$ . Note that the operator coefficient  $\widehat{\rho}^{(n)}(t)$  is time dependent whereas  $\widehat{H}^{(n)}$  is not. The definition of  $\widehat{H}^{(n)}$  is consistent with Eq. (12) and hence the  $\widehat{H}^F$  given in Eq. (51) is effectively similar to those discussed before.

Assuming that  $\hat{H}(t)$  is the total time-periodic Hamiltonian, one can partition the  $\hat{H}^F$  as

$$\hat{H}^F = \hat{H}_S^F \otimes \hat{I}_B + \hat{I}_S^F \otimes \hat{H}_B + \hat{H}_{SB}^F, \tag{54}$$

$$\hat{H}_{SB}^{F} = \sum_{i} \hat{C}_{i}^{\dagger} \hat{\mathcal{D}}_{i} + \text{H.c.}$$
 (55)

where  $\hat{I}_S^F = \hat{L}_0 \otimes \hat{I}_S$  and  $\hat{\mathcal{D}}_i = \hat{L}_0 \otimes \hat{d}_i$ . Then, we can define the following rotation protocols

$$\tilde{H}_{BS}^{F}(t) = e^{i\hat{H}_{B}t}e^{i\hat{H}_{S}^{F}t}\hat{H}_{BS}^{F}e^{-i\hat{H}_{B}t}e^{-i\hat{H}_{S}^{F}t}, \quad (56)$$

$$\tilde{\rho}(t) = e^{i\hat{H}_B t} e^{i\hat{H}_S^F t} \hat{\rho}(t) e^{-i\hat{H}_B t} e^{-i\hat{H}_S^F t}.$$
 (57)

The above rotations follow the transformation to the interaction picture in the context of conventional QME but, here within this version of Floquet QME, we have used  $\hat{H}_{S/SB}^F$ . Next, we can take the (initial factorization) assumption  $\tilde{\rho}^F(t) = \tilde{\rho}_S^F(t) \otimes \tilde{\rho}_B$  and proceed just as the conventional QME. This eventually leads to the following Floquet Markovian relation in the Schrödinger frame

$$\frac{\partial \hat{\rho}_{S}^{F}(t)}{\partial t} = -i \left[ \hat{H}_{S}^{F}, \hat{\rho}_{S}^{F}(t) \right] - \int_{0}^{\infty} \text{Tr}_{B} 
\left[ \hat{H}_{SB}^{F}, \left[ \tilde{H}_{SB}^{F}(\tau), \hat{\rho}_{S}^{F}(t) \otimes \hat{\rho}_{B} \right] \right] d\tau,$$
(58)

where  $\tilde{H}_{SB}^F(\tau) = e^{-i\hat{H}_B\tau}e^{-i\hat{H}_S^F\tau}\hat{H}_{SB}^Fe^{i\hat{H}_B\tau}e^{i\hat{H}_S^F\tau}$ . Because  $\hat{\rho}_S^F(t)$  is in the Floquet space, we can employ Floquet basis,  $\{|\gamma\rangle\}$ , to present elements of the reduced Floquet density operator (Floquet Hamiltonian) as  $\hat{\rho}_{S\gamma\nu}^F$ 

 $\langle \gamma | \hat{\rho}_S^F(t) | \nu \rangle$   $(H_{S\gamma\nu}^F(t) = \langle \gamma | \hat{H}_S^F | \nu \rangle)$ . After taking the integrations over  $\tau$  and employing Wide-band approximation, we arrive at the following matrix expression for the dynamic of the Floquet density matrix

$$\frac{\partial \rho_S^F(t)}{\partial t} = -i \left[ H_S^F, \rho_S^F(t) \right] - \sum_{i,j,l} \frac{\Gamma_{ij}^l}{2} \left( \mathcal{D}_i \widetilde{\mathcal{D}}_{jl}^\dagger \rho_S^F(t) + \mathcal{D}_i^\dagger \overline{\mathcal{D}}_{jl} \rho_S^F(t) - \mathcal{D}_i \rho_S^F(t) \widetilde{\mathcal{D}}_{jl}^\dagger - \mathcal{D}_i^\dagger \rho_S^F(t) \overline{\mathcal{D}}_{jl} \right) + \text{ h.c. },$$
(59)

where  $\widetilde{\mathcal{D}}_{jl}^{\dagger} = Y f_l(-\Omega) \circ \mathcal{D}_j^{\dagger} Y^{\dagger}$  and  $\overline{\mathcal{D}}_{jl} = Y f_l(\Omega) \circ \mathcal{D}_j Y^{\dagger}$ . The Floquet-Space FQME is thus easier to be implemented as compared to the Hilbert-Space FQME. The disadvantage of Floquet-Space FQME is that it requires more memory since all its components are in the Floquet space. Finally, we can simplify the notation of Eq. (59) as  $\partial \rho_S^F(t)/\partial t = -i \left[H_S^F, \rho_S^F(t)\right] + \sum_l \mathcal{L}_l^{FS} \rho_S^F(t)$ . Note that  $\mathcal{L}_l^{FS}$  is time-independent.

## G. Observable in Floquet QME

Within the Hilbert-Space FQME, it is straightforward to obtain expectation values of the particle number,  $\langle \hat{n} \rangle$  and current passing through the contact l,  $\langle \hat{J}_l \rangle$ , [38] as

$$\langle \hat{n} \rangle (t) = Tr(\hat{n}\hat{\rho}(t)),$$
 (60)

$$\langle \hat{J}_l \rangle (t) = Tr(\hat{n}\mathcal{L}_l^{HS}(t)\hat{\rho}(t)).$$
 (61)

To evaluate the expectation values of an observable in the Floquet-Space FQME, we need to project the operators from the Floquet space to the Hilbert space [11] as

$$\langle \hat{n} \rangle (t) = \sum_{m} Tr(\langle m | \hat{n}^F \hat{\rho}^F(t) | 0 \rangle e^{im\omega t}),$$
 (62)

$$\langle \hat{J}_l \rangle(t) = \sum_m Tr(\langle m | \hat{n}^F \mathcal{L}_l^{FS} \hat{\rho}^F(t) | 0 \rangle e^{im\omega t}).$$
 (63)

To evaluate  $\overline{n}$  and  $\overline{J}_l$  in both Floquet QME methods, we must evaluate the time-average of observables,  $\hat{O}(t)$ , numerically by using  $\overline{O} = 1/T \int_0^T \langle \hat{O} \rangle(t) dt$ .

# III. NUMERICAL RESULTS

To demonstrate the implications of light-matter interactions on the transport characteristics of an open quantum system, and to examine consistency between the discussed methods (V-like Floquet NEGF, M-like Floquet NEGF, Hilbert-Space FQME, and Floquet-Space FQME), we have first taken a spinless two-level quantum dot placed between two metallic contacts. This two-level dot then interacts with a monochromatic light. The one-body Hamiltonian of a such quantum dot can be given by

$$[h](t) = \begin{bmatrix} \varepsilon_1 & A\cos(\omega t) \\ A\cos(\omega t) & \varepsilon_2 \end{bmatrix}, \tag{64}$$

where  $\omega$  is the frequency of light and A represents the light intensity. Off-diagonal elements on the above Hamiltonian represent the dipole approximation in the context of light-matter interaction (Rabi model in quantum optics). This Hamiltonian is connected to the left (right) contacts with small  $\Gamma_{L(R)}$  (weak coupling regime). The schematic of such a configuration is given in Fig. 1.

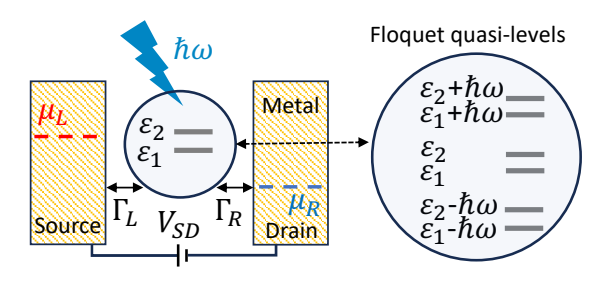


FIG. 1: (a) Schematics of a quantum transport system comprised of a two-level System under light illumination. The two-level System with monochromatic light can roughly be thought of as multiple quasi-levels.

## A. Results for Floquet NEGF methods

As the first example, we calculate the  $\overline{n}$  and  $\overline{J}_L$  (current passing through the left contact) using Eqs. (25-28) for a range of external bias,  $V_{SD} = \mu_R - \mu_L$  and multiple light frequencies. Hereafter, we will fix the right contact (Drain) at  $\mu_R = -0.4$  and sweep over  $\mu_L$ . In the absence of the light, and when off-diagonals of [h] are zero, there should be only two plateaus on the  $I-\mu_L$  curve such that the onset of these two plateaus are at  $\varepsilon_1$  and  $\varepsilon_2$ . When the A is large enough and the frequency of light is tuned to the difference between two levels,  $\hbar\omega = \varepsilon_2 - \varepsilon_1$ , then maximum alteration of the quantized conductance will happen such that the number of plateaus is doubled. This has been shown in Figs. 2(a) and 2(b). The extra quantized plateaus can be the hallmark of an electron-photon hybrid state (Floquet states). In extreme off-tuning situations (associated with  $\hbar\omega = 0.05$  and  $\hbar\omega = 0.4$ ), the transport characteristics should be almost identical to the non-Floquet transport characteristics. We can see it from the first and last curves in Figs. 2(a) and 2(b). At low frequencies, the M-like Floquet NEGF does not provide accurate results with only N=3. Hence, V-like Floquet NEGF delivers better numerical performance in low frequencies.

Next, we fixed the driving frequency at  $\hbar\omega=0.2~(eV)$  and calculated the two observables for a range of external bias,  $\mu_L$ , and multiple driving amplitudes, A. Results are plotted in Figs. 3(a) and 3(b). Here, we can see, that the light intensity, A, shifts the onset of plateaus symmetrically around  $\mu_L=0$ .

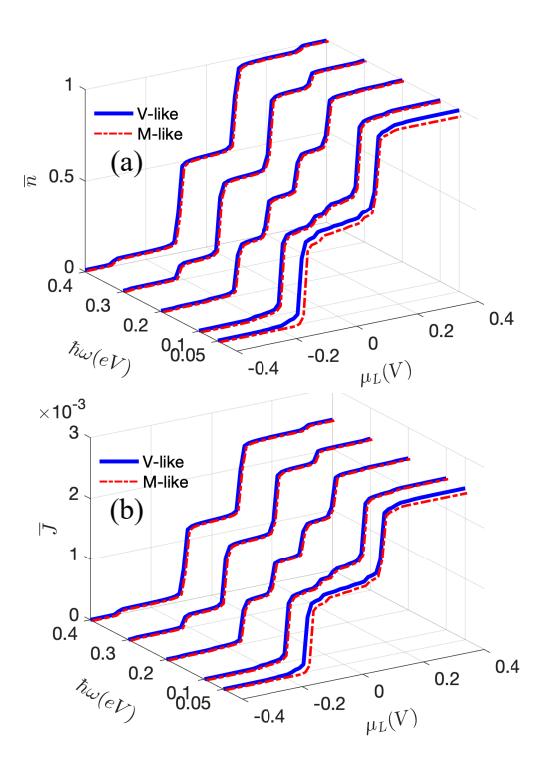


FIG. 2: Floquet NEGF: (a) One-period time-average of the number operator,  $\overline{n}$ , for multiple driving frequencies. Parameters are:  $\varepsilon_1 = -0.1~eV$ ,  $\varepsilon_2 = 0.1~eV$ , A = 0.1~eV, N = 3, T = 4.2~K,  $\Gamma_L = \Gamma_R = 0.0025~eV$ ,  $\mu_R = -0.4~V$ .

# B. Results for Floquet QME methods

We now use the spinless many-body operators  $d/d^{\dagger}$  to make the time-dependent many-body Hamiltonian and its Floquet counterpart. Then, by identifying the manybody basis set, an initial state (initial many-body density matrix), and the Fourier space (hence the many-body Floquet space), we will be able to perform dynamical solutions to Eqs. (47) and Eq. (59) and afterward evaluate time-averages of the observables, Eqs. (60)-(63). Note that, we have used the Runge-Kutta 4th-order method to solve Floquet QMEs. The time step has to be adjusted carefully. The rest of the parameters are the same as what is given in Fig. 2. The numerical cost of these solutions is much higher than the Floquet NEGF methods and hence, we only plotted the time averages of the number/current operator versus voltage for the perfect tuning case, (i.e.,  $\hbar\omega = 0.2 \ eV$ ) with the amplitude A = 0.1 (eV). Results are plotted in Fig. 4. To perform these calculations, we have considered the two-level system to be empty at t = 0 such that there will be no Rabi oscillation as time goes on. Firstly, we can see no pronounced oscillation in the  $\langle \hat{n} \rangle (t)$  of the Hilbert-Space FQME in the short-time limit [Fig. 4 (a)] whereas  $\langle \hat{n} \rangle (t)$  of the Floquet-Space FQME, shows oscillation fea-

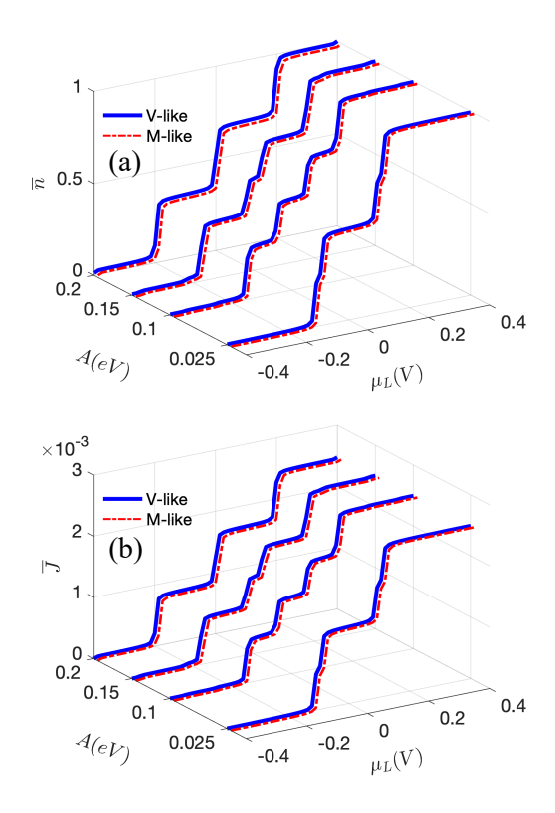


FIG. 3: Floquet NEGF: (a) One-period time-average of the number operator,  $\overline{n}$ , and (b) one-period time-average of the left contact's current operator,  $\overline{J}_L$ , for multiple driving amplitudes at  $\hbar\omega=0.2~(eV)$ . All other parameters are the same as Fig. 2.

ture [Fig. 4 (b)] in the early times. Such oscillations became steady as the time went by. Secondly, the two Floquet QME methods are identical in the long-time limit. Hence, calculated  $\overline{n}$ , and  $\overline{J}_L$  by the two Floquet QME is almost identical, see the solid and dashed lines in Figs. 4 (c) and (d). Thirdly,  $\overline{n}$ , and  $\overline{J}_L$  is also identical to the Floquet NEGF methods, compare Figs. 4 (c) and (d) with the central curves in Figs. 2 (a) and (b). Note that, we have found both Floquet QMEs require much smaller time steps as compared to the none Floquet QME. However, in comparison, the Hilbert-Space FQME is less sensitive to time step than the Floquet-Space FQME.

## C. Results for Floquet driven interacting system

Finally, we present a few numerical calculations performed for the spin case with and without interactions using the Floquet QME. When [U] and A (none-Floquet case) are both zero, having two spins, obviously, should result in the degeneracy factor 2 on the observed plateaus. In the presence of electron-electron interaction,  $[U] \neq 0$ , the number of plateaus increases such that the onset of the spin-up plateaus shifts with respect to

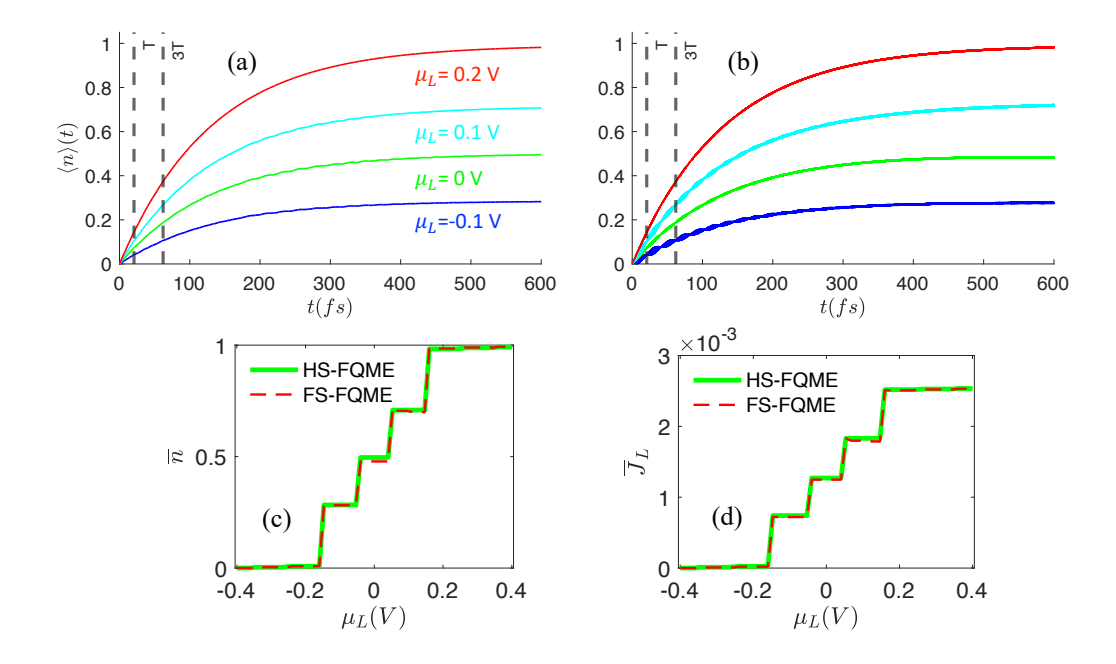


FIG. 4: Floquet QME: (a) time-dependent expectation value of the number operator evaluated by the Hilbert space Floquet QME. (b) Same as (a) evaluated by the Floquet space Floquet QME. (c) and (d) One-period time-average of the number operator, and the left contact's current operators,  $\overline{n}$ ,  $\overline{J}_L$ , at  $\hbar\omega=0.2~(eV)$  for a range of external bias. All other parameters are the same as Fig. 2.

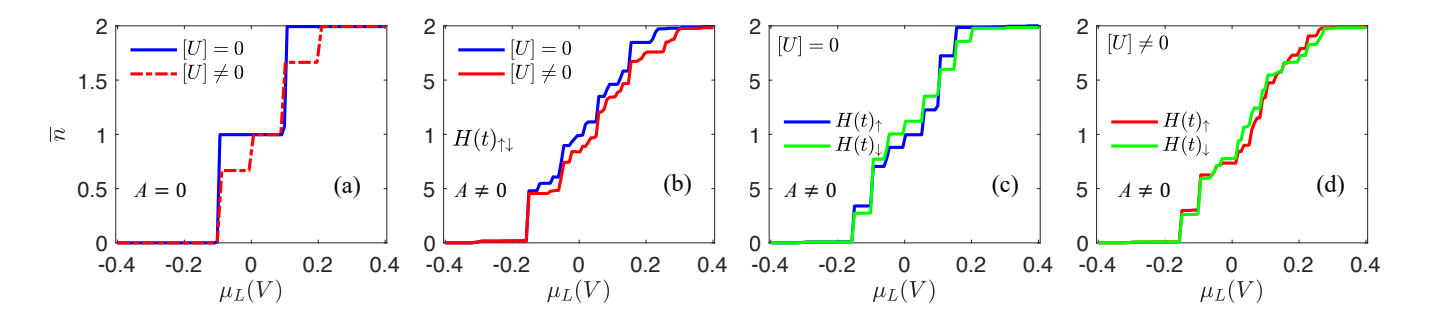


FIG. 5: Floquet QME for the interacting case: (a)  $\overline{n}$  vs the external bias when light is absent (A=0).  $[U] \neq 0$  gives rise to the extra quantized plateaus. We take  $u_1 = u_2 = 0.1$ , for the case where  $[U] \neq 0$ . All other parameters are the same as Fig. 4. (b)  $\overline{n}$  vs the external bias in the presence of light at  $\hbar\omega = 0.2$  (eV). (c) and (d) show  $\overline{n}$  vs the external bias when only dipole approximation is used in the time-periodic Hamiltonian.

the spin-down plateaus by the values  $\{u_i\}$  or vice versa. This observation is verified with our Floquet QME when A=0, see the dashed red line in Fig. 5 (a). The correct height ratio for the interacting case should be 2:1 [39]. Here in this section, we only show  $\overline{n}$  vs the external bias because  $\overline{J}$  follows the same pattern. Note that, the equation of motion technique in the NEGF, can reproduce the correct onsets for the plateaus however it does not often deliver the correct height for the plateaus. For a spin system and within the NEGF, we are required to include two identical time-dependent Hamiltonian, one for spin  $\downarrow$  and another for  $\uparrow$ , whereas, within the QME, we should only employ the spin version of many-body op-

erators  $\hat{d}/\hat{d}^{\dagger}$ . In Fig. 5 (b) we examined what will happen to the well-quantized plateaus of a two-level spin system subjected to a Floquet deriving with  $([U] \neq 0)$  and without two-body interaction ([U] = 0). Here, we include the dipole approximation for both spins [as indicated by  $H(t)_{\uparrow\downarrow}$ ]. We can see there is an interplay between the interaction and the Floquet driving such that even in the case of [U] = 0, the quantized Floquet plateaus of the spinless case do not simply multiply to the degeneracy factor 2. We can perceive that the electron-electron interaction in the presence of light, overall, lowers the population probability. To further speculate this interplay, we have evaluated  $\overline{n}$  vs the external bias when the

dipole approximation is taken into account only for one of the spins with and without interactions. Results of [U] = 0 and  $[U] \neq 0$  are plotted in Figs. 5 (c) and (d) respectively. Firstly, we can see the non-interacting spin system shows different quantization when only one spin is allowed to be excited. Secondly, electron-electron interaction makes the finer quantized population of the spin system smoother [compare Figs. 5 (c) with (d)].

#### IV. CONCLUSION

In the present work, we have derived four full Floquetbased formulations for the quantum transport through a time-periodic dot. In particular, we have shown the two Floquet Green's function formalisms rely on the expansion of Green's function, the first Floquet quantum master formalism, HS-FQME, relies on the Floquet time evolution operator, and the second Floquet quantum master formalism, FS-FQME relies on expanding the Hilbert space to the Floquet space. In addition, we have connected the equation of motion for each formulation to the time-averaged observables. Through a quantum dot model Hamiltonian, we quantitatively demonstrated that all Floquet quantum transport methods provide consistent results for non-interacting Hamiltonian in the weak coupling regime. The frequency and amplitude of time-periodic driving can significantly manipulate the time-average of observables. We have found an intense light can shift the one-set and the number of quantized plateaus in the voltage-current curve provided choosing an appropriate light frequency. As a drawback (even with parallel computation), we found Floquet quantum master equation frameworks to be computationally expensive. We also found that Floquet QME methods need much smaller time steps compared to the conventional QME. As usual with QME, when the lead-dot coupling or temperature decrease, the number of time step has to be increased. While the QME is the most practical method for interacting systems in the weak regime, it is computationally challenging to employ the full Floquet quantum master equation formalisms for large manybody systems. We believe the power of Floquet NEGF and Floquet QME methods goes well beyond the considered example and one needs to combine Floquet QMEs with newly developed machine learning methods to fully benefit from them.

## ACKNOWLEDGMENTS

This material is based upon work supported by the National Natural Science Foundation of China and (NSFC No. 22273075). V.M. acknowledges funding from the Summer Academy Program for International Young Scientists (Grant No. GZWZ[2022]019). W.D. acknowledges the startup funding from Westlake University.

#### CONFLICT OF INTEREST

There are no conflicts to declare.

# DATA AVAILABILITY STATEMENT

The data that support the findings of this study are available upon reasonable request from the authors.

<sup>[1]</sup> R. P. Feynman, *QED: The strange theory of light and matter*, Vol. 90 (Princeton University Press, 2006).

<sup>[2]</sup> H. Hübener, U. De Giovannini, C. Schäfer, J. Andberger, M. Ruggenthaler, J. Faist, and A. Rubio, Engineering quantum materials with chiral optical cavities, Nature materials 20, 438 (2021).

<sup>[3]</sup> S. He, L.-W. Duan, Y.-Z. Wang, C. Wang, and Q.-H. Chen, Quantum phase transition in the one-dimensional dicke-hubbard model with coupled qubits, Physical Review A 106, 033712 (2022).

<sup>[4]</sup> C. Gerry and P. L. Knight, *Introductory quantum optics* (Cambridge university press, 2005).

<sup>[5]</sup> M. F. Gelin, D. Egorova, and W. Domcke, Efficient calculation of time-and frequency-resolved four-wave-mixing signals, Accounts of chemical research 42, 1290 (2009).

<sup>[6]</sup> Y. Wang, H. Steinberg, P. Jarillo-Herrero, and N. Gedik, Observation of floquet-bloch states on the surface of a topological insulator, Science 342, 453 (2013).

<sup>[7]</sup> F. Mahmood, C.-K. Chan, Z. Alpichshev, D. Gardner, Y. Lee, P. A. Lee, and N. Gedik, Selective scattering between floquet-bloch and volkov states in a topological insulator, Nature Physics 12, 306 (2016).

<sup>[8]</sup> F. Faisal and J. Kamiński, Floquet-bloch theory of highharmonic generation in periodic structures, Physical Review A 56, 748 (1997).

<sup>[9]</sup> B. M. Fregoso, Y. Wang, N. Gedik, and V. Galitski, Driven electronic states at the surface of a topological insulator, Physical Review B 88, 155129 (2013).

<sup>[10]</sup> H. Sambe, Steady states and quasienergies of a quantummechanical system in an oscillating field, Physical Review A 7, 2203 (1973).

<sup>[11]</sup> K. L. Ivanov, K. R. Mote, M. Ernst, A. Equbal, and P. K. Madhu, Floquet theory in magnetic resonance: Formalism and applications, Progress in Nuclear Magnetic Resonance Spectroscopy 126, 17 (2021).

<sup>[12]</sup> S. Kohler, J. Lehmann, and P. Hänggi, Controlling currents through molecular wires, Superlattices and microstructures 34, 419 (2003).

<sup>[13]</sup> B. Wu and J. Cao, Noise of kondo dot with ac gate: Floquet-green's function and noncrossing approximation approach, Physical Review B 81, 085327 (2010).

<sup>[14]</sup> D. Rai and M. Galperin, Electrically driven spin currents in dna, The Journal of Physical Chemistry C 117, 13730 (2013).

- [15] Y. Su, Z.-H. Chen, H. Zhu, Y. Wang, L. Han, R.-X. Xu, and Y. Yan, Electron transfer under the floquet modulation in donor-bridge-acceptor systems, The Journal of Physical Chemistry A 126, 4554 (2022).
- [16] M.-B. Chen, B.-C. Wang, S. Kohler, Y. Kang, T. Lin, S.-S. Gu, H.-O. Li, G.-C. Guo, X. Hu, H.-W. Jiang, et al., Floquet state depletion in ac-driven circuit qed, Physical Review B 103, 205428 (2021).
- [17] S.-S. Gu, S. Kohler, Y.-Q. Xu, R. Wu, S.-L. Jiang, S.-K. Ye, T. Lin, B.-C. Wang, H.-O. Li, G. Cao, et al., Probing two driven double quantum dots strongly coupled to a cavity, Physical Review Letters 130, 233602 (2023).
- [18] B. Gu and I. Franco, Optical absorption properties of laser-driven matter, Physical Review A 98, 063412 (2018).
- [19] Y. Wang and W. Dou, Nonadiabatic dynamics near metal surface with periodic drivings: A floquet surface hopping algorithm, The Journal of Chemical Physics 158 (2023).
- [20] F. H. Faisal, Floquet green's function method for radiative electron scattering and multiphoton ionization in a strong laser field, Computer Physics Reports 9, 57 (1989).
- [21] G. Stefanucci, S. Kurth, A. Rubio, and E. Gross, Time-dependent approach to electron pumping in open quantum systems, Physical Review B 77, 075339 (2008).
- [22] N. Tsuji, T. Oka, and H. Aoki, Correlated electron systems periodically driven out of equilibrium: Floquet+dmft formalism, Physical Review B 78, 235124 (2008).
- [23] G. Cabra, I. Franco, and M. Galperin, Optical properties of periodically driven open nonequilibrium quantum systems, The Journal of chemical physics **152** (2020).
- [24] K. Szczygielski, On the application of floquet theorem in development of time-dependent lindbladians, Journal of mathematical physics 55 (2014).
- [25] A. K. Eissing, V. Meden, and D. M. Kennes, Functional renormalization group in floquet space, Physical Review B 94, 245116 (2016).
- [26] U. Peskin, Formulation of charge transport in molecular junctions with time-dependent molecule-leads coupling operators, Fortschritte der Physik 65, 1600048 (2017).
- [27] A. Schnell, A. Eckardt, and S. Denisov, Is there a floquet lindbladian?, Physical Review B 101, 100301 (2020).

- [28] Z. N. Qaleh and A. Rezakhani, Enhancing energy transfer in quantum systems via periodic driving: Floquet master equations, Physical Review A 105, 012208 (2022).
- [29] G. Engelhardt, G. Platero, and J. Cao, Discontinuities in driven spin-boson systems due to coherent destruction of tunneling: breakdown of the floquet-gibbs distribution, Physical Review Letters 123, 120602 (2019).
- [30] G. Engelhardt and J. Cao, Dynamical symmetries and symmetry-protected selection rules in periodically driven quantum systems, Physical review letters 126, 090601 (2021).
- [31] G. Engelhardt, S. Choudhury, and W. V. Liu, Unified light-matter floquet theory and its application to quantum communication, arXiv preprint arXiv:2207.08558 (2022).
- [32] G. Cohen and M. Galperin, Green's function methods for single molecule junctions, The Journal of chemical physics 152 (2020).
- [33] J. H. Shirley, Solution of the schrödinger equation with a hamiltonian periodic in time, Physical Review 138, B979 (1965).
- [34] T. Mori, Floquet states in open quantum systems, Annual Review of Condensed Matter Physics 14, 35 (2023).
- [35] S. Datta, Quantum Transport: Atom to Transistor (Cambridge University Press, 2005).
- [36] A.-P. Jauho, N. S. Wingreen, and Y. Meir, Timedependent transport in interacting and noninteracting resonant-tunneling systems, Physical Review B 50, 5528 (1994).
- [37] D. A. Ryndyk et al., Theory of quantum transport at nanoscale, Springer Series in Solid-State Sciences 184, 9 (2016).
- [38] U. Harbola, M. Esposito, and S. Mukamel, Quantum master equation for electron transport through quantum dots and single molecules, Physical Review B 74, 235309 (2006).
- [39] N. A. Zimbovskaya, Electron transport through a quantum dot in the coulomb blockade regime: nonequilibrium green's function based model, Physical Review B 78, 035331 (2008).